Available online at www.sciencedirect.com
SCIENCE DIRECT®
Journal of Nuclear Materials 329–333 (2004) 338–341
journal of nuclear materials
www.elsevier.com/locate/jnucmat

Nanometer scale precipitation in ferritic MA/ODS alloy MA957

M.K. Miller *, D.T. Hoelzer [1], E.A. Kenik [2], K.F. Russell [3]

Metals and Ceramics Division, Oak Ridge National Laboratory, P.O. Box 2008, Oak Ridge, TN 37831-6136, USA

Abstract

The microstructure of a commercial mechanically-alloyed oxide dispersion strengthened MA957 alloy has been characterized in the as-received condition and after annealing for up to 24 h at 1300 °C (~0.85 T_m) by atom probe tomography and electron microscopy. Atom probe tomography revealed a high number density of ultrafine 2-nm-diameter Ti-, Y- and O-enriched particles in the ferrite matrix in the as-received condition. The size increased and the number density of these particles decreased during the annealing treatment for 1 and 24 h at 1300 °C. Some coarser (~10 nm) Ti-, Y- and O-enriched precipitates were also observed at the grain boundaries. No significant grain growth or recrystallization was observed during the high temperature annealing treatment.
Published by Elsevier B.V.

1. Introduction

The oxide dispersion strengthened (ODS) MA957 ferritic steel was developed in the late 1970s for liquid-metal fast breeder reactors due to the excellent high temperature creep and tensile properties [1,2]. The use of ODS ferritic steels is also attractive for fusion reactor applications because of their potential for higher operating temperatures and for trapping helium at the dispersed oxide particles. Some similar tungsten-containing mechanically-alloyed ODS ferritic alloys (designated 12YWT) have shown remarkable improvement in their creep properties at temperatures up to 850 °C compared to the molybdenum-containing MA957 alloy [3–7]. The intragranular microstructure of the 12YWT alloy was found to contain a high number density of ultrafine Ti-, Y- and O-enriched particles that were resistant to coarsening during high temperature creep or isothermal annealing at up to 1300 °C [8–13]. The purpose of this study was to investigate the nanometer scale microstructure in the MA957 with atom probe tomography to determine whether this molybdenum-containing alloy also exhibited similar ultrafine Ti-, Y- and O-enriched particles and to determine the stability of the nanometer size particles during high temperature annealing treatments close to the melting point of the alloy.

2. Experimental

The commercial MA957 alloy used in this study had a nominal composition of Fe–14 wt% Cr, 0.9% Ti, 0.3% Mo, and 0.25% Y_2O_3 [Fe–14.8 at.%Cr, 0.17% Mo, 1.0% Ti, 0.13% Y and 0.19% O] and contained trace levels of Al, Mn, Si, B and C. Atom probe and transmission electron microscopy specimens were cut from an extruded tube and electropolished into suitable specimens. This alloy was characterized in the as-received state and after annealing for up to 24 h at 1300 °C (~0.85 T_m).

The ultrafine scale microstructure and solute distribution of the MA/ODS alloy was characterized by atom probe tomography [14]. The atom probe tomography characterizations were performed in the Oak Ridge National Laboratory's (ORNL) energy-compensated optical position-sensitive atom probe (ECOPOSAP).

* Corresponding author. Tel.: +1-865 574 4719; fax: +1-865 241 3650.
E-mail address: millermk@ornl.gov (M.K. Miller).
[1] Tel.: +1-865 574 5096; fax: +1-865 241 3650.
[2] Tel.: +1-865 574 5066; fax: +1-865 241 3650.
[3] Tel.: +1-865 576 7676; fax: +1-865 241 3650.

0022-3115/$ - see front matter Published by Elsevier B.V.
doi:10.1016/j.jnucmat.2004.04.085

The experiments were performed with a specimen temperature of 50–60 K, pulse repetition rates of 1.5 kHz, and a pulse fraction of 20% of the standing voltage. All compositions quoted in this paper are expressed in atomic percent. The Guinier radius, r_G, and the composition of each particle were determined from the positions of the solute atoms associated with the particles with the use of the maximum separation method. The parameters used were a maximum solute separation distance of 0.6 nm and a grid spacing of 0.1 nm [14]. Transmission electron microscopy and scanning electron microscopy were also used to study the dislocation structure of the alloy and to determine whether recrystallization had occurred during the high temperature anneal.

3. Results

The general microstructures of the MA957 alloy in the as-received condition and after isothermal aging at 1300 °C are shown in the optical micrographs in Fig. 1. The MA957 alloy exhibited a uniform microstructure of elongated grains, some cavities and a low number density of micron-sized particles. Transmission electron microscopy (TEM) analyses revealed that these coarse micron-sized particles were the Al_2O_3 phase. Formation and coarsening of the cavities occurred during the annealing treatment at 1300 °C. TEM observations also revealed some fine (~10 nm diameter) Ti-, Y- and O-enriched particles along the grain boundaries, as shown in Fig. 2. TEM analyses revealed partial recovery of the dislocation structure but no recrystallization had occurred during the high temperature anneal. No significant grain growth was observed in either of the annealed conditions.

Atom probe tomography revealed a high number density ($\sim 2\times10^{24}$ m^{-3}) of ultrafine Ti-, Y- and O-enriched particles in the ferrite matrix of the as-received condition, as shown in the atom maps in Fig. 3. The average Guinier radius of these intragranular particles was determined with the use of the maximum separation method [14] to be 1.2 ± 0.4 nm. The average composition of these particles in the as-received condition was

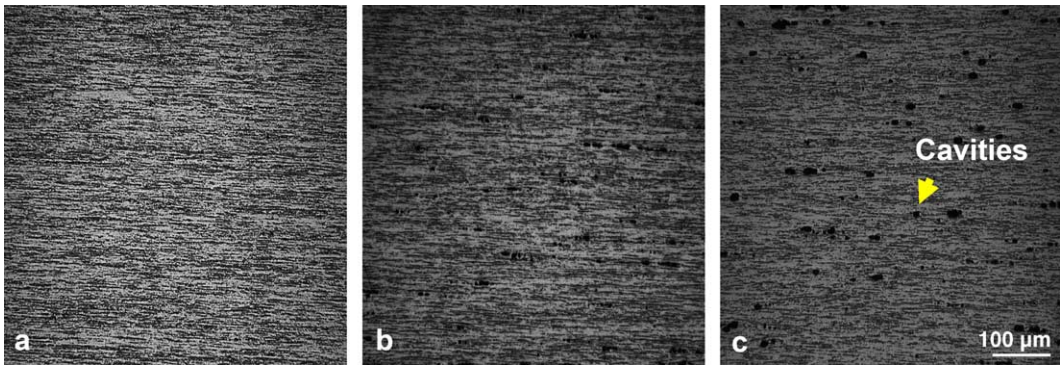

Fig. 1. Optical micrographs of the general microstructure of MA957 in the (a) as- received condition and after annealing for (b) 1 h at 1300 °C and (c) 24 h at 1300 °C.

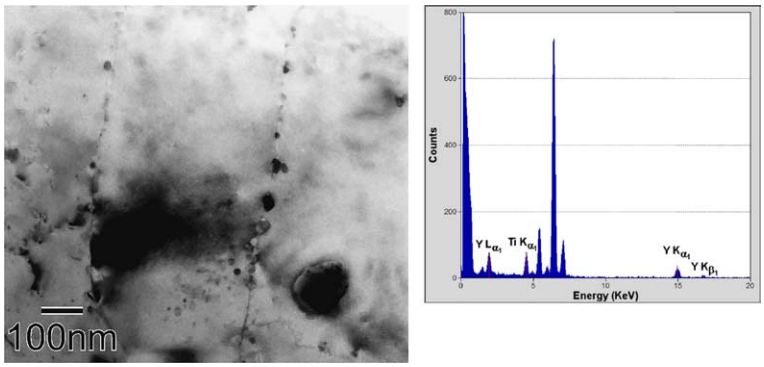

Fig. 2. TEM micrograph and an energy-dispersive spectroscopy spectra of Ti-, Y- and O-enriched particles along grain boundaries in the MA957 alloy.

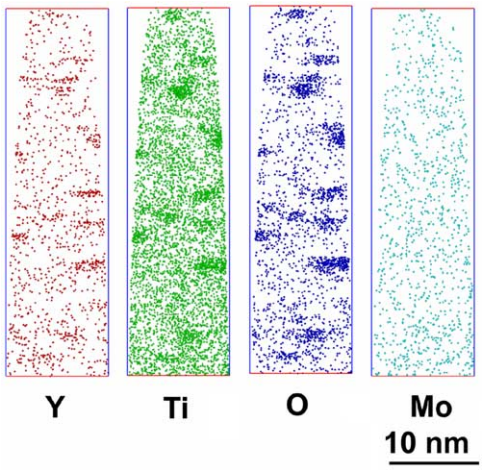

Fig. 3. Atom maps showing titanium-, oxygen- and yttrium-enriched particles in the as-received MA957 alloy.

estimated by the envelope method [14] to be Fe–32.9 ± 5.3 at.% Ti, 15.4 ± 7.3% Y, 39.9 ± 6.9% O, 1.7 ± 1.7% Cr, and 0.02 ± 0.2% Mo. The oxygen content in the ferrite matrix was estimated to be less than 0.14 ± 0.04 at.% O for the as-received condition. The number density of these particles decreased significantly from $\sim 2\times10^{24}$ to $\sim 2\times10^{23}$ m^{-3} after annealing for 1 h at 1300 °C and to $\sim 8\times10^{22}$ m^{-3} after annealing for 24 h

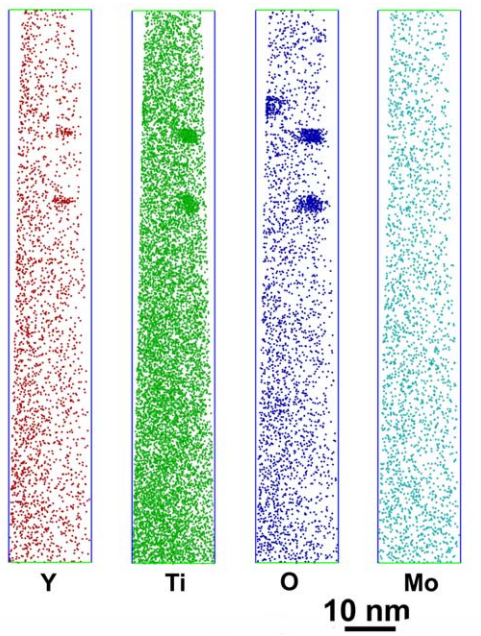

Fig. 4. Atom maps showing titanium-, oxygen- and yttrium-enriched particles in the MA957 alloy after annealing for 1 h at 1300 °C.

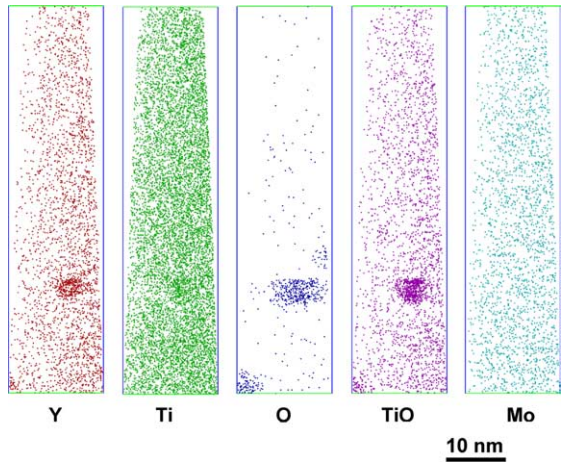

Fig. 5. Atom maps showing titanium-, oxygen- and yttrium-enriched particles in the MA957 alloy after annealing for 24 h at 1300 °C. Most of the titanium and oxygen field evaporates as TiO^{2+} ions.

at 1300 °C. The Guinier radius of the particles increased to 1.7 ± 0.4 and 4.6 ± 1.1 nm after annealing for 1 and 24 h at 1300 °C, respectively. The average composition of these particles after annealing for 1 h at 1300 °C was estimated to be Fe–21.3 ± 7.9 at.% Ti, 8.9 ± 5.8% Y, 47.8 ± 23.3% O, 4.2 ± 4.2% Cr, and 0.03 ± 0.1% Mo and the oxygen in the matrix was 0.16 ± 0.07 at.% O Fig. 4. These results indicate that some coarsening of the particles had occurred during the high temperature anneal however, a significant number of particles were still present after annealing for 24 h at 1300 °C, as shown in the atom maps in Fig. 5.

4. Discussion

The high titanium and relatively low yttrium and oxygen contents of these particles indicate that they are not remnants of the original yttria powder. Therefore, the main function of mechanical alloying appears to break up the yttria particles and to force the yttrium and oxygen into supersaturated solid solution in the ferrite matrix despite the thermodynamic stability of yttria.

In order for the Ti-, Y- and O-enriched particles to coarsen, all the solute elements associated with the particles (i.e., the yttrium, titanium and oxygen) have to dissolve from the surface of the smaller particles, diffuse in the ferrite matrix, and to deposit on the surface of the larger particles. Since titanium and yttrium atoms are significantly larger than iron atoms, it could be inferred that these elements may diffuse slowly in an iron lattice. However, this large misfit may be alleviated by solute-vacancy interactions and it is possible that a titanium-

vacancy and a yttrium-vacancy may diffuse significantly more rapidly than isolated solute atoms.

The oxygen content of the ferrite was found to be significantly higher than the parts per million expected from previous estimates of the solubility in ferrite [15]. The majority of the titanium and oxygen atoms both in the particles and the matrix were detected as TiO molecular ions in the atom probe, as shown in Fig. 5, together with a lower proportion of CrO and YO ions. The presence of these molecular ions indicates a strong affinity of oxygen for the solute atoms since these molecular ions are uncommon in atom probe analyses. This affinity is somewhat expected due to the large heats of formation of all the oxide phases. In order for the oxygen and the other solute elements to diffuse in the ferrite, the solute-oxygen bond either has to be broken, or the solute-oxygen complex has to diffuse as an entity. Since neither of these processes is energetically favorable, the strong solute-oxygen affinity may retard or even inhibit the diffusion process. In addition, the strong solute-oxygen affinity may be the reason for the high oxygen content in the ferrite due to trapping.

The solute distribution in the intragranular regions and the formation of the ultrafine Ti-, Y- and O-enriched particles in this MA957 alloy are similar to those found in previous atom probe tomography characterizations of 12YWT alloys indicating that the molybdenum or tungsten additions do not significantly change the intragranular precipitation in MA/ODS ferritic alloys. However, the Ti-, Y- and O-enriched particles had coarsened slightly more in this MA957 alloy as compared to the 12YWT alloy. This trend is consistent with the free energies of formation of the molybdenum and tungsten oxides. In addition, the molybdenum concentration in the MA957 alloy (0.17 at.%) is lower than the tungsten level (0.92 at.%) in the 12YWT alloy thereby providing a lower number of less efficient trapping sites. Therefore, molybdenum may not be as effective as tungsten in retarding the coarsening process. This difference in coarsening rate may also contribute to the inferior creep properties of the MA957 alloy compared to the 12YWT alloy.

5. Conclusions

Atom probe tomography has revealed the formation of the ultrafine (2-nm-diameter) Ti-, Y- and O-enriched particles in the matrix of a commercial MA957 in the as-received condition. These particles were found to coarsen slightly during isothermal annealing for 24 h at 1300 °C. A high oxygen content was measured in the ferrite matrix. The lower molybdenum content in MA957 was found to be less effective in trapping oxygen at solute atoms than the higher tungsten content in 12YWT alloys and therefore, was not as effective in retarding the coarsening of the Ti-, Y- and O-enriched particles during high temperature annealing.

Acknowledgements

Research at the Oak Ridge National Laboratory SHaRE Collaborative Research Center was sponsored by the Division of Materials Sciences and Engineering and the Office of Nuclear Energy, Science and Technology (I-NERI 2001-007-F), US Department of Energy, under contract DE-AC05-00OR22725 with UT-Battelle, LLC.

References

[1] J.J. Fischer, Dispersion strengthened ferritic alloy for use in liquid-metal fast breeder reactors (LMFBRS), US Patent 4,075,010 issued 21 February 1978.
[2] G.D. Smith, J.J. deBarbadillo, in: J.J. deBarbadillo et al. (Eds.), Structural Applications of Mechanical Alloying, ASM-International, Materials Park, OH, 1994, p. 117.
[3] S. Ukai, M. Harada, H. Okada, M. Inoue, S. Nomura, S. Shikakura, K. Asabe, T. Nishida, M. Fujiwara, J. Nucl. Mater. 204 (1993) 65.
[4] S. Ukai, M. Harada, H. Okada, M. Inoue, S. Nomura, S. Shikakura, T. Nishida, M. Fujiwara, J. Nucl. Mater. 204 (1993) 74.
[5] S. Ukai, T. Nishida, H. Okada, T. Okuda, M. Fujiwara, K. Asabe, J. Nucl. Sci. Technol. 34 (1997) 256.
[6] S. Ukai, T. Yoshitake, S. Mizuta, Y. Matsudaira, S. Hagi, T. Kobayashi, J. Nucl. Sci. Technol. 36 (1999) 710.
[7] I.-S. Kim, T. Okuda, C.-Y. Kang, J.-H. Sung, P.J. Maziasz, R.L. Klueh, K. Miyahara, Met. Mater. 6 (2000) 513.
[8] D.J. Larson, P.J. Maziasz, I.-S. Kim, K. Miyahara, Scr. Mater. 44 (2001) 359.
[9] I.-S. Kim, J.D. Hunn, N. Hashimoto, D.J. Larson, P.J. Maziasz, K. Miyahara, E.H. Lee, J. Nucl. Mater. 280 (2000) 264.
[10] E.A. Kenik, D.T. Hoelzer, P.J. Maziasz, M.K. Miller, Microsc. Microanal. 7 (2001) 550.
[11] M.K. Miller, E.A. Kenik, Microsc. Microanal. 8 (Suppl. 2) (2002) 1126CD.
[12] M.K. Miller, E.A. Kenik, K.F. Russell, L. Heatherly, D.T. Hoelzer, P.J. Maziasz, Mater. Sci. Eng. A 353 (2003) 140.
[13] M.K. Miller, D.T. Hoelzer, E.A. Kenik, K.F. Russell, Microsc. Microanal. 9 (Suppl. 2) (2003) 44.
[14] M.K. Miller, Atom Probe Tomography, Kluwer Academic/Plenum, New York, 2000.
[15] J.H. Swisher, E.T. Turkdogan, Trans. Met. Soc. AIME 239 (1967) 426.